Temporal Map Formation in the Barn Owl's Brain

Christian Leibold, Richard Kempter, and J. Leo van Hemmen
Physik Department, Technische Universität München, 85747 Garching bei München, Germany
(Received 19 March 2001; published 27 November 2001)

Barn owls provide an experimentally well-specified example of a temporal map, a neuronal representation of the outside world in the brain by means of time. Their laminar nucleus exhibits a place code of interaural time differences, a cue which is used to determine the azimuthal location of a sound stimulus, e.g., prey. We analyze a model of synaptic plasticity that explains the formation of such a representation in the young bird and show how in a large parameter regime a combination of local and nonlocal synaptic plasticity yields the temporal map as found experimentally. Our analysis includes the effect of nonlinearities as well as the influence of neuronal noise.

DOI: 10.1103/PhysRevLett.87.248101 PACS numbers: 87.18.–h, 43.64.+r, 87.19.La

Many animals have in their brain neuronal representations of the outside world, which we call *maps*. These representations are due to sensory organs. Vision, for instance, provides a direct map through the lens of the eye onto the retina and, accordingly, is dominantly spatial. Audition, on the other hand, has far fewer cues but time is one of them, a very important one. Here we face the question of how a temporal map can arise and provide an answer by considering a specific example, the barn owl's sound localization.

Barn owls are nocturnal predators that are able to catch mice in complete darkness. In so doing they reach an amazing azimuthal resolution of 2°. Interaural (inter-ear) time differences have been shown [1] to be their only cue. The spatial resolution implies a temporal precision at least as good as 40 μs [2,3].

We focus on the laminar nucleus as the first station in the brain receiving input from *both* ears. Interaural time differences (ITDs) are represented there by means of a *place code*. That is to say, the azimuthal position is mapped one-to-one onto corresponding neuronal sites in the laminar nucleus, each neuron signaling its preferred azimuthal location through a maximal firing rate. As the stimulus location is varied, so is the maximal ITD response in the laminar nucleus [2]; cf. Fig. 1. Henceforth the resulting map is a neuronal representation of *azimuthal* stimulus locations. We can now ask two questions. How does it function, in particular, why is the precision that good (40 μs), and how does it arise? As we will see, the answers to both questions are interrelated in that the map as it evolves leads to firing precision.

Here we analyze how a novel mechanism of synaptic plasticity [5] gives rise to a temporal map. As was indicated by a numerical study [5], local so-called Hebbian learning depending on spike timing of the pre- and postsynaptic neuron [6,7], which precede and follow the synapse under consideration (hence Hebbian), and small, axonally propagated, synaptic modifications [8] together induce a temporal map. One may call the underlying mechanism "axon-mediated spike-based learning" (AMSL). We now present an analytic solution to the proposed synaptic dynamics and explain the model's performance in dependence upon the learning procedure, biological constraints, and neuronal noise.

The basic, though often questioned, idea of an ITD map dates back to Jeffress [9]. He proposed an array of coincidence-detector cells with a topology as the one in Fig. 1; we return to it in Fig. 4. If, at a specific neuron, the difference of conduction delays between the axon bundles originating from left and right ear compensates for the acoustic time difference that occurs between both ears

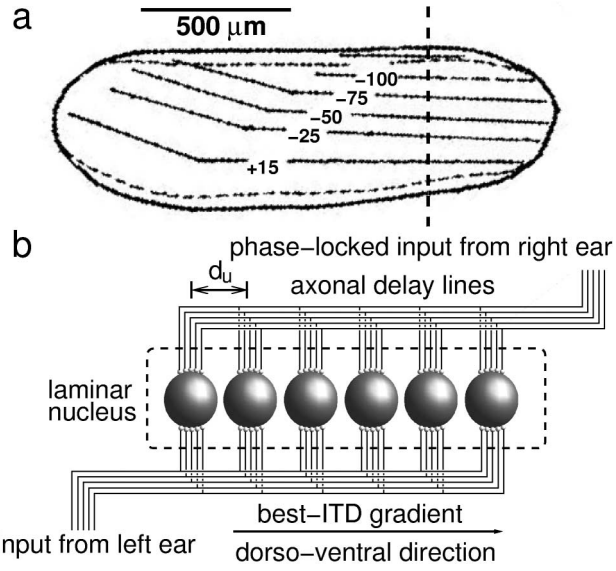

FIG. 1. (a) Interaural time difference (ITD) map in a barn owl's laminar nucleus, after Sullivan and Konishi [4]. Iso-ITD contours (solid lines) consist of neurons with maximal response at ITDs as indicated; e.g., −25 corresponds to the left ear leading by 25 μs. The vertical dashed line is the cut shown in (b), where neuronal activity is conveyed by spike trains in axon bundles (thin lines) that come from left and right ear, run in parallel to the dorso-ventral direction (arrow), and contact neurons through synapses (small white balls). Measuring firing rates of neurons (large grey spheres) along this direction, one finds the neuronal site where the firing rate is maximal to vary continuously with the stimulus angle. Neurons are taken to be equidistant with $d_u = 10$ μm, a typical value.

and is caused by the sound source location, then the cell receives spikes that are temporally highly correlated and thus [10] fires at high rate. In the young animal each axon carries phase-locked input but the temporal dispersion of all spikes arriving at each neuron [2] has a width of 1 ms, i.e., one to several periods of the frequencies involved (1–9 kHz). We now show why nonetheless Jeffress was right. In so doing we exploit that temporal (in)coherence of spike arrival leads to synaptic potentiation (depression) and in this way to a selection of axonal delays.

The spike-generating potential v_m of laminar neuron m ($1 \le m \le M$) is taken to be [11] a sum of postsynaptic potentials ϵ of the form as in Fig. 2(a), and

$$v_m(t) = \sum_{n=1}^{N} J_{mn} \sum_{t_n^f} \epsilon(t - t_n^f - \Delta_{mn}) . \qquad (1)$$

Here the input spikes are generated at times t_n^f and delayed through axon $1 \le n \le N$ by Δ_{mn}. The coefficients J_{mn} are called synaptic weights and act as dynamical variables for map formation.

Axonal selection is implemented by means of a learning rule depending on spike timing initiated by (1) but such [5] that a synapse-specific weight change $(\frac{d}{dt} J_{mn})_{\text{local}}$, due to pre- and postsynaptic spikes at the very same synapse, also has a small effect on all other ($m' \neq m$) synaptic weights $J_{m'n}$ connected to the *same* axon n. The total change dJ_{mn}/dt is then given by

$$\frac{d}{dt} J_{mn} = \sum_{m' \in \text{axon } n} (\delta_{mm'} + \rho) \left(\frac{d}{dt} J_{m'n} \right)_{\text{local}} , \qquad (2)$$

where ρ is small and positive, say $0.01 < \rho < 0.1$.

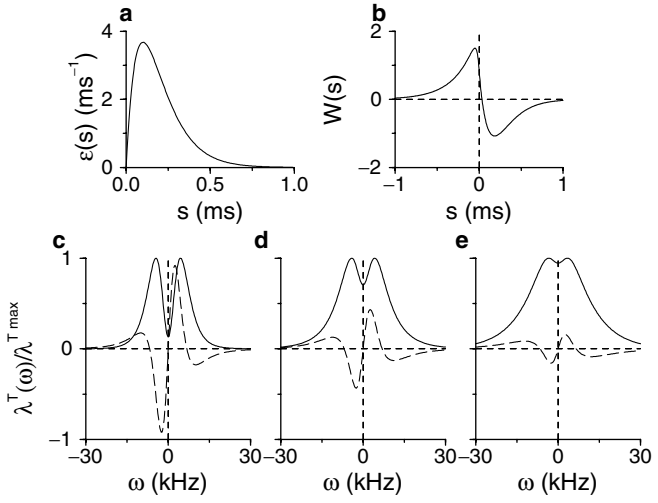

FIG. 2. Excitatory postsynaptic potential $\epsilon(s) = s/\tau^2 \times \exp(-s/\tau)$ for $s \ge 0$, $\epsilon(s) = 0$ for $s < 0$ with $\tau = 0.1$ ms (a) and learning window W [5] (b), as they have been used in numerical simulations. The normalized temporal eigenvalues $\lambda^{\mathrm{T}} \propto \hat{W}^{\text{eff}} \hat{\epsilon}^{\text{eff}}$ for $\beta J^{\text{fix}} = 0$ (c), 1/3 (d), and 2/3 (e) show bandpass properties. Real parts (solid lines) get broader as β increases, whereas imaginary parts (dashed lines) approach zero.

The local dynamics is governed by a Hebbian term that involves the temporally averaged correlation function $C_{mn}(t, t')$ between pre- and postsynaptic spike trains. In addition, it has two stabilizing terms involving the temporally averaged pre- and postsynaptic firing rates ν_n^{in} and ν_m^{out}, respectively,

$$\left(\frac{d}{dt} J_{mn} \right)_{\text{local}} = \eta \Big[w^{\text{in}} \nu_n^{\text{in}} + w^{\text{out}} \nu_m^{\text{out}} + \int_{-\infty}^{\infty} ds\, W(s) C_{mn}(t, t + s - \Delta_{mn}) \Big] . \qquad (3)$$

This equation is exact as long as $0 < \eta \nu \mathcal{T} \ll 1$ for firing rates ν and times $\mathcal{T}$ as they often occur in praxis, typical changes of J_{mn} being too small to effect the momentary neuronal dynamics [12,13]. The integral kernel W of the correlation term in (3) is meanwhile widely known as the learning window [6,7]; cf. Fig. 2(b).

In order to specify ν^{in}, ν^{out}, and C in Eq. (3), we take an inhomogeneous Poisson process [10] that is suitable for modeling the input spike trains stemming from acoustic stimulation. Since the auditory system is tonotopically organized, i.e., different frequency components of a sound are processed at different locations of the basilar membrane, the array of Fig. 1(b) is preferentially exposed to input with one prominent period T_p.

At least at the neuronal time scale of ϵ and W [see Figs. 2(a) and 2(b)], it is justified to deal with a periodic input process whose intensity [10] is defined through $p^{\text{in}}(t) = p g(t)$ where $\int_0^{T_p} ds\, g(s) = 1$ and $p = \nu^{\text{in}} T_p$ adjusts the process to a mean firing rate ν^{in}. Since the distribution of delays at the borders of the laminar nucleus Δ_{0n} is about 1 ms wide, ITD-sensitive neurons have best frequencies $1/T_p \ge 1$ kHz, and we consider delays $\bmod T_p$, we put $\Delta_{0n} = n T_p/N$ with $1 \le n \le N$. With N between 100 and 1000, equidistant delays are a good approximation to a homogeneous distribution [2] so that $\Delta_{mn} = \Delta_{0n} + m d_u/c$. Here $c \approx 5$ m/s denotes the axonal conduction velocity; cf. Fig. 1(b).

The explicit shapes of both the correlation function C and the postsynaptic rate ν^{out} are a direct consequence of the neuron model. In the present work, we use Poisson neurons [10–13] whose firing probability density p_{F} is a function of the instantaneous membrane potential $v(t)$. The probability that a neuron fires once during $[t, t + \Delta t)$ is $p_{\mathrm{F}}[v(t)]\Delta t$; firing twice or more has a probability $o(\Delta t)$, while the events in disjoint intervals are taken to be independent. Here we take

$$p_{\mathrm{F}}[v(t)] = \nu_0 \exp[-\beta v(t)] . \qquad (4)$$

A more general formulation will be given elsewhere.

The resulting dynamics $d\mathbf{J}/dt = \mathcal{N}(\mathbf{J})$ is nonlinear in $\mathbf{J} = \{J_{mn}\}$. To solve this nonlinear problem we proceed as follows. First, we show that, under rather general conditions, $J_{mn}^{\text{fix}} = J^{\text{fix}} = \text{const}$ is a fixed-point configuration,

i.e., $\mathcal{N}(\mathbf{J}^{\rm fix}) = 0$. Second, we linearize the dynamics about the fixed point and analyze the system's temporal evolution by means of a spectral analysis of the first derivative $D\mathcal{N}$ [13–15].

With $\mathbf{J} = \mathbf{J}^{\rm fix}$, the mean firing rate is constant in time and independent of the position m of the laminar neuron,

$$\nu^{\rm out} = \nu_0 \exp\left\{N\nu^{\rm in}\int_0^\infty ds[\exp(\beta J^{\rm fix}\epsilon(s)) - 1]\right\}. \quad (5)$$

The correlation function is independent of time,

$$C_{mn}(t + r, t) = \nu^{\rm out}\nu^{\rm in}\exp[\beta J^{\rm fix}\epsilon(r - \Delta_{mn})]. \quad (6)$$

The fixed-point equation $\mathcal{N}(\mathbf{J}^{\rm fix}) = 0$ gives

$$\frac{\nu^{\rm out}}{\nu^{\rm in}} = \frac{-w^{\rm in}}{\nu^{\rm in}\int ds\, W^{\rm eff}(s, \beta J^{\rm fix}) + w^{\rm out}} =: \gamma, \quad (7)$$

where the effective learning window is defined to be $W^{\rm eff}(s, x) := W(s)\exp[x\epsilon(-s)]$. In neuronal networks the ratio γ between input and output rate is of order 1. An arbitrary value of $\gamma > 0$ can be obtained by adjusting $w^{\rm in}$ and $w^{\rm out}$ in (7), whatever the value of $\nu^{\rm in}$ and $\beta J^{\rm fix}$. We thus postulate a fixed positive value γ and, due to (5), we can write

$$\frac{\ln(\gamma\nu^{\rm in}/\nu_0)}{N\nu^{\rm in}} = \int_0^\infty ds\{\exp[\beta J^{\rm fix}\epsilon(s)] - 1\}, \quad (8)$$

which we define to be $\psi(\beta J^{\rm fix})$. Here ψ is a monotonically increasing function of $\beta J^{\rm fix}$ with $\psi(0) = 0$. Hence, for $\ln(\gamma\nu^{\rm in}/\nu_0) > 0$, there is a unique fixed-point solution $\beta J^{\rm fix}$.

Linearizing the equations of motion makes sense as the negative spectrum tells us what the domain of attraction looks like. Furthermore, typical initial conditions can be shown to be here. Hence the system first approaches the fixed point before the "positive" eigendirections take over. The linearized differential equation reads in the neighborhood of the fixed point

$$\frac{d}{dt}\iota_{mn} = \tilde{\eta}\sum_{m'n'}(\delta_{mm'} + \rho)(k + Q_{nn'})\iota_{m'n'}, \quad (9)$$

where $\tilde{\eta} = \eta\beta\nu^{\rm out}\nu^{\rm in}$. This is just a rewriting of $d\boldsymbol{\iota}/dt = D\mathcal{N}\boldsymbol{\iota}$. Defining the effective response kernel $\epsilon^{\rm eff}(s, x) := \epsilon(s)\exp[x\epsilon(s)]$ and Fourier transform $\hat{f}_\mu := \int ds\, f(s)e^{-2\pi i\mu/T_p s}$, we find $k = w^{\rm out}\hat{\epsilon}_0^{\rm eff}$ and

$$Q_{nn'} = \nu^{\rm in}\sum_{\mu=-\infty}^{\infty}|\hat{g}_\mu|^2\hat{\epsilon}_\mu^{\rm eff}\hat{W}_\mu^{\rm eff}e^{2\pi i\mu/T_p(\Delta_{mn}-\Delta_{mn'})}. \quad (10)$$

$Q_{nn'}$ does not depend on m since due to a *constant* axonal conduction velocity $c \approx 5$ m/s [2] the delay difference $\Delta_{mn} - \Delta_{mn'} = \Delta_{0n} - \Delta_{0n'}$ between axon n and n' is independent of the position m of the laminar neuron. Hence Eq. (9) is *separable* in space (m) and time (Δ_{0n}) so that eigenfunctions $\boldsymbol{\phi}$ and eigenvalues λ are products of a spatial and a temporal component, viz., $\phi_{mn} = \phi_m^{\rm S}\phi_n^{\rm T}$ with $\lambda = \lambda^{\rm S}\lambda^{\rm T}$.

We now turn to structure formation. The spatial eigenvalue with largest real part $\lambda^{\rm S} = 1 + \rho M$ belongs to the constant vector $\phi_m^{\rm S} = 1$, whereas the temporal eigenvalue $\lambda^{\rm T} = \tilde{\eta}\nu^{\rm in}|\hat{g}_\mu|^2\hat{\epsilon}_\mu^{\rm eff}\hat{W}_\mu^{\rm eff}$ with the largest real part has to be determined through an analysis of the Fourier components $\hat{\epsilon}_\mu^{\rm eff}\hat{W}_\mu^{\rm eff}$; see Figs. 2(c)–2(e). For sufficiently high $\omega = 2\pi/T_p$ (the minimal best frequency of laminar neurons is about 1 kHz, which yields $\omega = 6$ kHz), we find the maximal real part for $\mu = \pm 1$ and, therefore, in the Δ_{mn}-m plane of Fig. 3, the prominent eigenvector is $\phi_{mn} = \exp(2\pi i\Delta_{mn}/T_p)$, which is consistent with numerical simulations [5] and explains experimental findings [2].

Let us imagine that, after a few days of learning, the learning rule (2) has produced the synaptic structure that is shown in Fig. 3. Then the ensemble-averaged membrane potential $\langle v_m(t)\rangle$ is a standing wave, with wavelength $cT_p/2$. The neuronal position of maximal amplitude is determined by the phase difference Φ between input from the left and right ears. As is indicated in Fig. 4, we have obtained a *place code* representing the interaural time difference $T_p\Phi/(2\pi)$. Because of the (nonlinear) firing probability given by (4), the standing-wave amplitudes of the neuronal input (1) are transformed into spikes, hence firing rates, and yield a place code of sound-stimulus azimuth as found in experiment [2,4] and shown in Fig. 1(a). A neuronal timing precision as good as 40 μs is a direct consequence of the synaptic delay selection [6].

Imaginary parts of eigenvalues of the operator $D\mathcal{N}$ in (9) lead to oscillations and are as such disadvantageous to structure formation. A closer look at Figs. 2(c)–2(e) reveals, however, that imaginary parts are suppressed by increasing β. That is to say, nonlinearities in $p_{\rm F}$ can stabilize synaptic learning.

Another interesting result of the present analysis is that the axonal interaction strength ρ contributes to the spatial eigenvalue $\lambda^{\rm S}$ as $1 + \rho M$. In other words, $\rho \approx 1/M$ already affects the synaptic dynamics distinctly. There is experimental evidence [8] that such contributions may indeed be very weak.

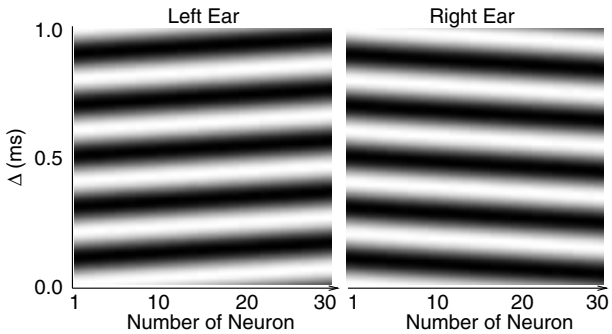

FIG. 3. The leading eigenvector of the operator $D\mathcal{N}$ from Eq. (9), for a 5 kHz input, an axonal conduction velocity of 5 m/s [2], and $d_u = 10$ μm distance between neighboring neurons. The eigenvectors of left- and right-ear afferents differ by the direction of spike conduction. They give a temporal map as in Fig. 1(a); Δ is to be taken mod T_p.

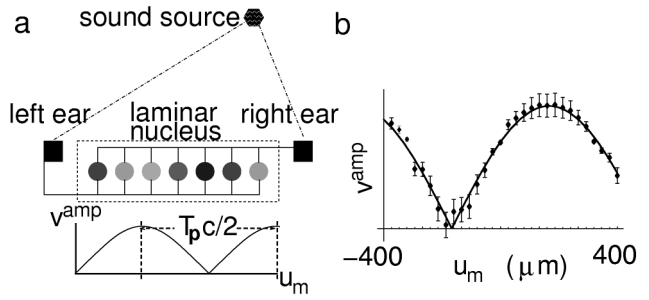

FIG. 4. Coincidence detector array of neurons (grey shaded circles) as proposed by Jeffress [9]. Auditory stimuli are transduced to cells in the barn owl's laminar nucleus. They are delayed by (i) the spatial distance between the sound source and the ears (dot-dashed lines) and (ii) the physiological conduction from the ear to the cell (solid lines). In reality, many more axons than one are involved. After delay tuning, the averaged membrane potential $\langle v(t)\rangle = v_0 + v_1 \cos(\omega_p u_m/c + \Phi)\cos(\omega_p t)$ is a standing wave across the laminar nucleus with wavelength $cT_p/2$, and constants $v_{0/1}$ depending on the choice of parameters. Its phase Φ is defined by the interaural time difference. The azimuthal position of the sound source in auditory space is thus mapped onto the position u_m of *maximal* amplitude $v^{\text{amp}} = |v_1 \cos(\omega_p u_m/c + \Phi)|$ of the membrane potential within the laminar nucleus. The brighter the circle, the higher the membrane potential amplitude. (b) For comparison, we show the simulated amplitude of the membrane potential (dots with error bars) and its theoretical prediction (solid line) for an ITD of 50 μs, interaction parameter $\rho = 0.7/30$, and synaptic weights after 875 s of formal learning time. Other parameter values have been taken from Kempter *et al.* [5].

In spite of that, one might argue the higher ρ the faster structure formation. This holds true as long as Eq. (2) is valid. Since, however, it is an ensemble-averaged equation we have to investigate the effect of ρ on the standard deviation and, hence, the variance of the trajectory of J_{mn} due to jittery spike input and output. We obtain [12]

$$\text{Var}(J_{mn})(t) = t[(1 + \rho M)^2 D_1 + (1 + 2\rho + \rho^2 M) D_2 + \mathcal{O}(N^{-1/2})], \quad (11)$$

where D_1 and D_2 are of order $\mathcal{O}(\eta^2)$ and give the diffusion constant $D := t^{-1}\text{Var}(J_{mn})$. In this way we find the time scale of weight changes evoked by input noise to be of the order of $(J^{\text{fix}})^2/D$ and end up with two scenarios. Both follow from the requirement that terms involving ρ in (11) be of order 1.

First, if $D_1 \gtrsim D_2$, the leading power of the interaction terms in (11) is $(\rho M)^2$. Therefore $\rho \lesssim M^{-1}$ gives a constraint for the order of magnitude of the interaction parameter. A number of, e.g., $M = 30$ postsynaptic cells, which is roughly the number of neurons along the ITD gradient in the laminar nucleus, yields $\rho \lesssim 3\%$ as a maximum for the axonal interaction. Second, if $D_1 \ll D_2$ the leading power is $\rho^2 M$, which yields an upper limit $\rho \lesssim M^{-1/2}$. Hence for $M = 30$ we get the condition $\rho \lesssim 18\%$. An *in vitro* experiment on hippocampal cells [8] suggests $\rho \approx 1\%$.

In conclusion, the present work shows how the formation of an interaural time-difference map depends on an interplay of the parameters of the learning rule, such as the shape of the learning window and the non-Hebbian contributions w^{in} and w^{out}, and neuronal properties, such as the shape of the response kernel and the firing-probability density. In particular, we have proven that an unspecific axonal modification of order $\rho \approx \mathcal{O}(1/M)$ is sufficient for map formation. We have also shown how nonlinearities in spike generation stabilize synaptic learning and, with Eq. (7), we have given an explicit expression that relates the quotient of input and output rate of map neurons to the parameters characterizing their synaptic learning rule. In so doing we have recovered the temporal map as it occurs in the laminar nucleus of the mature barn owl. Further along the auditory pathway, the two "one-dimensional" interaural intensity level difference and ITD maps are combined [16] so as to give a mental representation of the prey's position in spherical coordinates (θ, ϕ).

The authors thank Catherine Carr and Hermann Wagner for supplying a wealth of biological information on barn owls. R. K. and C. L. have been supported by the Deutsche Forschungsgemeinschaft (DFG) and the State of Bavaria, respectively.

[1] A. Moiseff, J. Comp. Physiol. A **164**, 629 (1989).
[2] C. E. Carr and M. Konishi, J. Neurosci. **10**, 3227 (1990).
[3] C. Köppl, J. Neurosci **17**, 3312 (1997).
[4] W. E. Sullivan and M. Konishi, Proc. Natl. Acad. Sci. U.S.A. **83**, 8400 (1986).
[5] R. Kempter, C. Leibold, H. Wagner, and J. L. van Hemmen, Proc. Natl. Acad. Sci. U.S.A. **98**, 4166 (2001).
[6] W. Gerstner, R. Kempter, J. L. van Hemmen, and H. Wagner, Nature (London) **383**, 76 (1996); S. Song, K. D. Miller, and L. F. Abbott, Nat. Neurosci. **3**, 919 (2000).
[7] L. I. Zhang, H.-z. W. Tao, C. E. Holt, W. A. Harris, and M.-m. Poo, Nature (London) **395**, 37 (1998).
[8] H.-z. W. Tao, L. I. Zhang, G.-q. Bi, and M.-m. Poo, J. Neurosci. **20**, 3233 (2000); S. Cash, R. S. Zucker, and M.-m. Poo, Science **272**, 998 (1996); R. M. Fitzsimonds, H.-J. Song, and M.-m. Poo, Nature (London) **388**, 439 (1997).
[9] L. A. Jeffress, J. Comp. Physiol. Psychol. **41**, 35 (1948).
[10] R. Kempter, W. Gerstner, and J. L. van Hemmen, and H. Wagner, Neural Comput. **10**, 1987 (1998), App. A.
[11] W. Gerstner and J. L. van Hemmen, in *Models of Neural Networks II,* edited by E. Domany, J. L. van Hemmen, and K. Schulten (Springer, New York, 1994), pp. 1–93.
[12] R. Kempter, W. Gerstner, and J. L. van Hemmen, Phys. Rev. E **59**, 4498 (1999).
[13] J. L. van Hemmen, in *Handbook of Biological Physics,* edited by F. Moss and S. Gielen (Elsevier, Amsterdam, 2001), Vol. 4, pp. 771–823.
[14] D. J. C. MacKay and K. D. Miller, Network **1**, 257 (1990).
[15] C. W. Eurich, K. Pawelzik, U. Ernst, J. D. Cowan, and J. G. Milton, Phys. Rev. Lett. **82**, 1594 (1997).
[16] J. L. Peña and M. Konishi, Science **292**, 249 (2001).